Bull. Mater. Sci., Vol. 34, No. 6, October 2011, pp. 1179–1183. © Indian Academy of Sciences.

Chemical synthesis and characterization of hydrous tin oxide (SnO_2:H_2O) thin films

S N PUSAWALE, P R DESHMUKH and C D LOKHANDE*
Department of Physics, Shivaji University, Kolhapur 416 004, India

MS received 17 November 2010; revised 11 April 2011

Abstract. In the present investigation, we report chemical synthesis of hydrous tin oxide (SnO_2:H_2O) thin films by successive ionic layer adsorption and reaction (SILAR) method at room temperature (∼300 K). The films are characterized for their structural and surface morphological properties. The formation of nanocrystalline SnO_2 with porous and agglomerated particle morphology is revealed from X-ray diffraction (XRD) and scanning electron microscopy (SEM) studies, respectively. The Fourier transform infrared spectroscopy (FTIR) study confirmed the formation of Sn–O phase and hydrous nature of the deposited film. Static water contact angle studies showed the hydrophilic nature of SnO_2:H_2O thin film. Electrical resistivity showed the semiconducting behaviour with room temperature electrical resistivity of 10^5 Ω cm. The electrochemical properties studied in 0·5 M Na_2SO_4 electrolyte showed a specific capacitance of 25 F g^{-1} at 5 mVs^{-1} scan rate.

Keywords. Thin films; chemical synthesis; hydrous tin oxide; FTIR; electrical properties.

1. Introduction

In recent years, synthesis of hydrous metal oxide thin films for supercapacitor application is attracting much more attention. Among the various metal oxides, hydrous form of RuO_2 showed much higher specific capacitance of 788 F g^{-1} (Park *et al* 2004a, b) than its anhydrous form, which is about 58 F g^{-1} (Subramanian *et al* 2004). This high specific capacitance value is mainly due to the proton intercalation in the bulk material of hydrous RuO_2 (Burke *et al* 1977; Michell *et al* 1978; Burke and Whelan 1979; Zheng *et al* 1995). However, due to the high cost of RuO_2 precursors, it cannot be used for commercial applications. Therefore, extensive research is being carried out on the synthesis of inexpensive hydrous metal oxides including hydrous MnO_2 and hydrous (Co–Ni)O_2. Among the various hydrous metal oxides, hydrous form of tin oxide (SnO_2:H_2O) has been previously studied as a selective catalyst in the oxidative dehydrogenation of organic compounds (Hattori *et al* 1987). SnO_2 electrode has shown promising supercapacitive properties, however, no studies on the electrochemical properties of hydrous SnO_2 have been reported.

In an earlier report, the SnO_2:H_2O has been prepared from the precipitation of Sn containing acidic or alkaline solutions using a soluble base (Kostrikin *et al* 2007). In the present work, we have used successive ionic layer adsorption and reaction (SILAR) method for deposition of SnO_2:H_2O thin films. The method has great advantage of depositing hydrous metal oxide thin films at sufficiently low temperature. It is a nonelectrical method, so the particles in the solution can be in suspension state; due to this, the method allows the deposition of nanolayers and nanoclusters of hydrous metal oxides on the substrate surface. The SILAR method is simple and inexpensive, which comprises excellent material utilization efficiency, good control over deposition process along with film thickness and convenient for large area deposition on virtually any type of substrate (Pathan and Lokhande 2004; Tolstoy 2006).

In the present investigation, for the first time, we report on the synthesis of SnO_2:H_2O thin films by SILAR method. The SnO_2:H_2O thin films are characterized for their structural, surface morphological, electrical and electrochemical properties.

2. Experimental

SnO_2:H_2O thin films were deposited by SILAR method on glass and stainless steel substrates. For the deposition, cationic precursor was 0·05 M tin (II) chloride ($SnCl_2 \cdot 2H_2O$) as a source of Sn^{4+} ions. The anionic precursor was 1% H_2O_2 solution. Both the cationic and anionic precursors were kept at room temperature (∼300 K). One SILAR cycle consists of two steps: (i) adsorption of Sn^{4+} ions on the substrate surface for 20 s and (ii) reaction with H_2O_2 solution for 40 s to form stable SnO_2:H_2O thin film on the substrate.

The structural property of SnO_2:H_2O films was studied using a Philips (PW-3710) X-ray diffractometer with a Cr Kα (λ = 2·2870 Å) target. FTIR spectrum of the

*Author for correspondence (l_chandrakant@yahoo.com)

sample was obtained using Perkin Elmer, FTIR spectrum one unit. The microstructure of the film was observed using scanning electron microscopy (JEOL, JEM-6360, Japan). Static water contact angle measurement was carried out using Rame–Hart Instrument Co., USA equipped with a CCD camera. Film roughness was measured using computerized AMBIOS make XP-1 surface profiler with 1 Å vertical resolution. Electrical resistivity was measured by d.c. two-point probe method. Electrochemical study was performed in a three-electrode configuration cell consisting of SnO_2:H_2O as a working electrode, platinum as a counter electrode and saturated calomel electrode (SCE) as a reference electrode.

3. Results and discussion

3.1 *Film formation mechanism and thickness measurement*

The mechanism of formation of SnO_2:H_2O film can be elucidated as follows. The $SnCl_2$ solution gives Sn^{4+} ions (Chang *et al* 2005). In aqueous acidic solution, Sn^{4+} ions hydrolyze to form $Sn(OH)_4$ which precipitates on the substrate surface immersed in it.

$$Sn^{4+} + 4H_2O \rightarrow Sn(OH)_4 + 4H^+. \quad (1)$$

The substrate with $Sn(OH)_4$ formed on its surface is then rinsed in dilute H_2O_2 solution, where formation of SnO_2:H_2O takes place through the following reaction

$$Sn(OH)_4 + H_2O_2 \rightarrow SnO_2 : H_2O + 2H_2O + \frac{1}{2}O_2 \uparrow . \quad (2)$$

This completes one cycle for formation of SnO_2:H_2O monolayer. Several such cycles were repeated to achieve terminal film thickness. Thickness of the SnO_2:H_2O film was measured by a gravimetric weight difference method in terms of the weight of SnO_2:H_2O deposited on the substrate per unit area, since accurate measurement of SnO_2:H_2O film thickness was not possible due to rough morphology and porosity of the film (Park *et al* 2004a, b). The graph of the weight of SnO_2:H_2O thin film deposited with deposition cycles is shown in figure 1. The weight of the film increased with the increase in number of deposition cycles from 25 to 75. After 75 cycles, the decreased weight of film probably may be due to the peeling off of the powdery material from the substrate surface. The terminated weight at which highest amount of SnO_2:H_2O deposited on stainless steel substrate surface was 0·22 mg cm^{-2}.

3.2 *Structural studies*

Figure 2(a, b) shows the X-ray diffraction patterns of bare glass substrate and SnO_2:H_2O thin film on glass substrate. From figure 2(a) absence of diffraction peaks confirms the amorphous nature of glass substrate. The presence of broad, small and well distinct peaks observed for SnO_2:H_2O in figure 2(b) indicate the formation of nanocrystalline material. The peaks at $2\theta = 39{\cdot}8°$, $51{\cdot}1°$ and $80{\cdot}54°$ correspond to the (110), (101), and (211) planes of cassiterite SnO_2 (JCPDS card no. 77-0452). The calculated lattice parameters '*a*' and '*c*' of the cassiterite SnO_2:H_2O are 4·750 Å and 3·196 Å, respectively matching well with the standard values. The crystallite size is calculated for (110) plane using Scherrer's formula

$$d = \frac{0{\cdot}9\lambda}{\beta \cos\theta}, \quad (3)$$

where d is the crystallite size, β the full width at half maxima, λ the wavelength of X-ray used and θ the diffraction angle. SnO_2:H_2O film has an average crystallite size of about 15 nm, confirming the nanosize of deposited material.

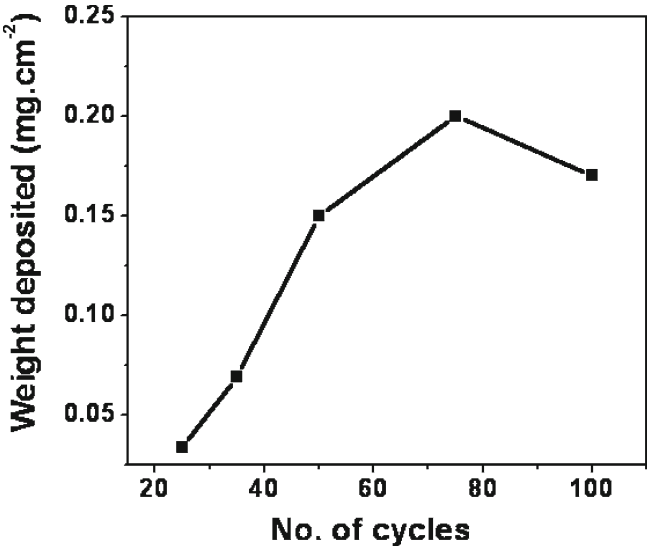

Figure 1. Variation of weight of SnO_2:H_2O thin film deposited with number of deposition cycles.

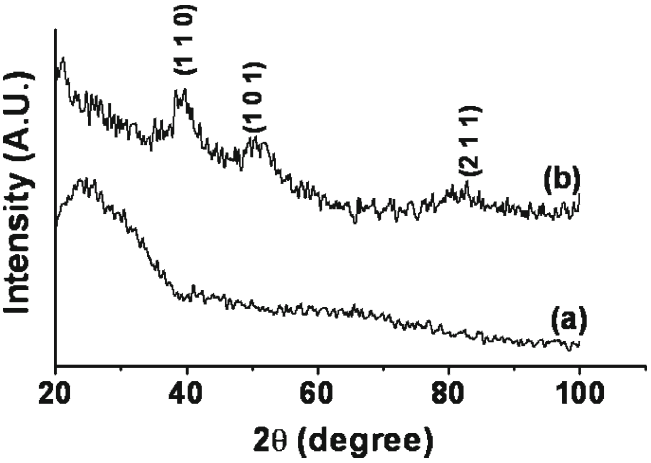

Figure 2. XRD patterns of (**a**) bare glass substrate and (**b**) SnO_2:H_2O thin film on glass substrate.

3.3 *FTIR studies*

Figure 3 shows FTIR spectrum of SnO_2:H_2O thin film in the range 400–4000 cm^{-1}. FTIR study confirmed the formation of SnO_2 with characteristic vibrational mode of Sn–O at 579 cm^{-1} (Abello *et al* 1998). The peak at 1142 cm^{-1} is due to the δ (SnOH) vibrations (Abello *et al* 1998). The hydrous nature of SnO_2 is confirmed from the peak at 1640 cm^{-1}, which is due to the bending vibration of hydroxyl groups of molecular water (Wang and Herron 1991). The absorption peak at 3377 cm^{-1} indicates the presence of hydroxide group (Karuppuchamy and Jeong 2006) due to the deposition from an aqueous bath.

3.4 *Surface morphological studies*

Figure 4(a, b) shows SEM micrographs of stainless steel substrate without and with deposition of SnO_2:H_2O thin film at ×10,000. The smooth surface stainless steel is observed from SEM image. With the deposition of SnO_2:H_2O, the non-uniform spherical grains covering entire surface of the stainless steel substrate is observed. The agglomeration of the nanoparticles forms large crystallites. These crystallites are non-uniform and irregularly arranged, constructing the porous morphology. Such morphology provides large surface area and finds application as a supercapacitor electrode (Pell and Conway 2001; Yang *et al* 2007; Li *et al* 2008).

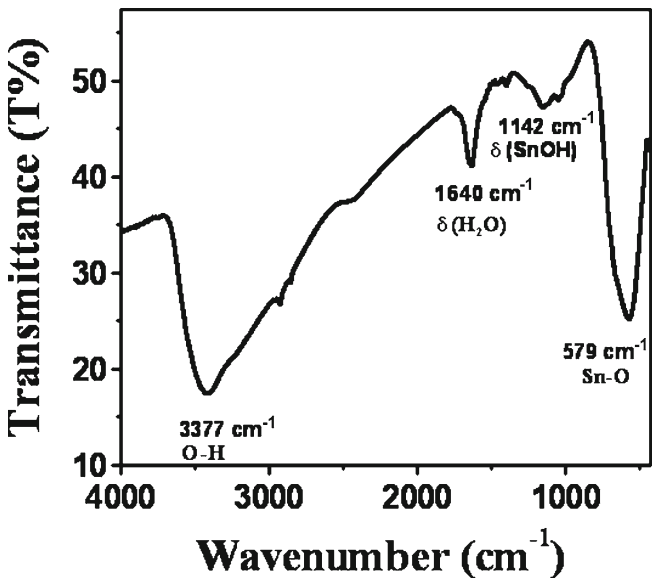

Figure 3. FTIR spectrum of SnO_2:H_2O thin film.

Table 1. Variation of surface roughness and contact angle values of SnO_2:H_2O thin film with number of deposition cycles.

No. of deposition cycles	Deposited weight (mg cm^{-2})	Roughness (Å)	Contact angle (°)
25	0·03	2071	12
35	0·07	2245	15
50	0·15	2678	17
75	0·22	6438	20

3.5 *Surface wettability studies*

Surface wettability involves the interaction between liquid and solid in contact. The wettability of the solid surface can be classified as hydrophobic (water hating) or hydrophilic (water loving); depending upon the contact angle made by water on the solid surface is greater or less than 90°, respectively. The water contact angle observed for bare stainless steel substrate is 9° which shows its hydrophilic nature. The variation of contact angle with deposited weight of SnO_2:H_2O is summarized in table 1, which gives the values of surface roughness and water contact angle for variation in deposited weight of SnO_2:H_2O film. It is observed that the contact angle is increased from 12 to 20° with increase in roughness. It is proposed that for the better performance of supercapacitors, the hydrophilic surface of the electrode is one of the important factors for better insertion of electrolyte within the pores of the electrode material (Bockman *et al* 2000).

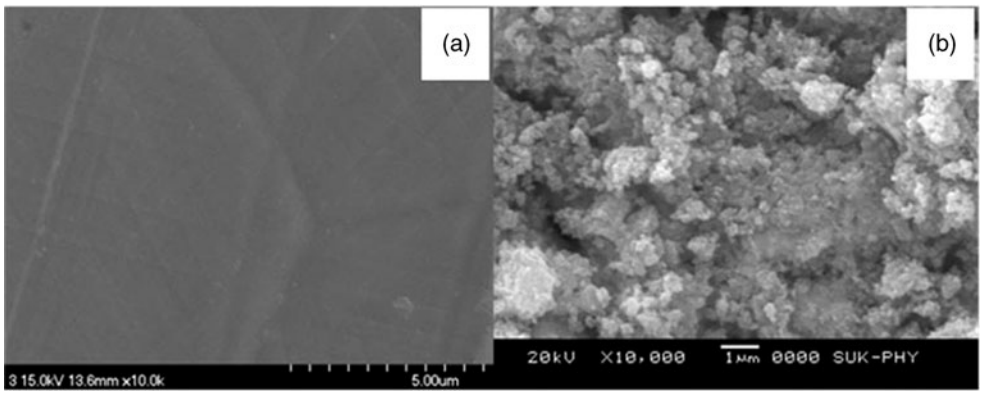

Figure 4. SEM images of (**a**) bare stainless steel and (**b**) SnO_2:H_2O thin film on stainless steel substrate at a magnification of ×10,000.

3.6 *Electrical resistivity*

The variation of d.c. electrical resistivity with weight deposited of SnO_2:H_2O thin film is studied in the temperature range from 300 to 500 K using two-point probe method. The variation of (logρ) with reciprocal temperature (1000/T) is depicted in figure 5. The resistivity was decreased from 10^7 to 10^5 Ω cm as the weight deposited increased from 0·07 to 0·22 mg cm^{-2}. The resistivity of the film decreased with increase in temperature, indicating semiconducting behaviour. For the SnO_2:H_2O thin films with deposited weights of 0·15 and 0·22 mg cm^{-2}, we observed transition from a straight-line region with a low gradient to one with a higher gradient as temperature is increased above 350–370 K. This suggests that more than one conduction mechanism is involved (Dhawale *et al* 2008). For the SnO_2:H_2O film with a weight of 0·15 mg cm^{-2}, the activation energies are 0·14 and 0·69 eV in low and high temperature regions, respectively which are 0·27 and 0·69 for the film with a weight of 0·22 mg cm^{-2}.

3.7 *Electrochemical studies*

The electrochemical properties of SnO_2:H_2O film deposited on stainless steel substrate are studied in 0·5 M Na_2SO_4 in the voltage range of ±500 mV vs SCE at 50 mV s^{-1} scan rate. Figure 6(a) shows the cyclic voltammogram (C–V) of bare stainless steel electrode with negligible current response. The increase in current is observed only after the deposition of SnO_2:H_2O film on stainless steel substrate, which confirms that the current is originating from SnO_2:H_2O material. Figure 6(b–d) shows the C–V curves for different deposited

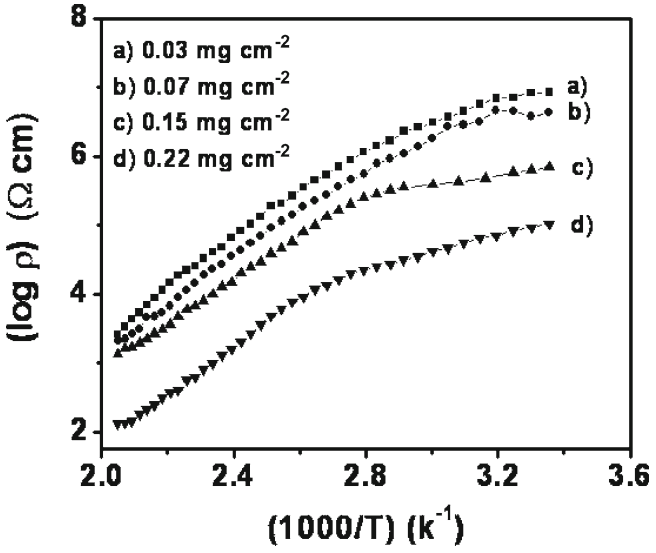

Figure 5. Variation of electrical resistivity (log ρ) with temperature (1000/T) of SnO_2:H_2O films for (**a**) 0·03, (**b**) 0·07, (**c**) 0·15 and (**d**) 0·22 mg cm^{-2} weights.

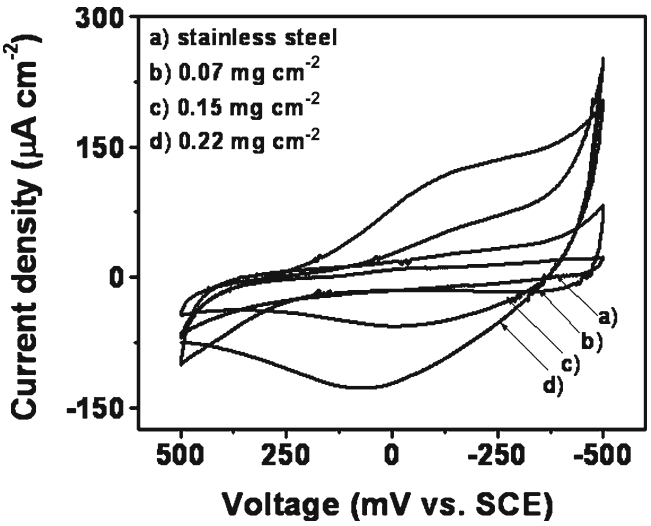

Figure 6. Cyclic voltammograms at 50 mV s^{-1} in 0·5 M Na_2SO_4 electrolyte for (**a**) bare stainless steel electrode and SnO_2:H_2O electrode for (**b**) 0·07, (**c**) 0·15 and (**d**) 0·22 mg cm^{-2} weights.

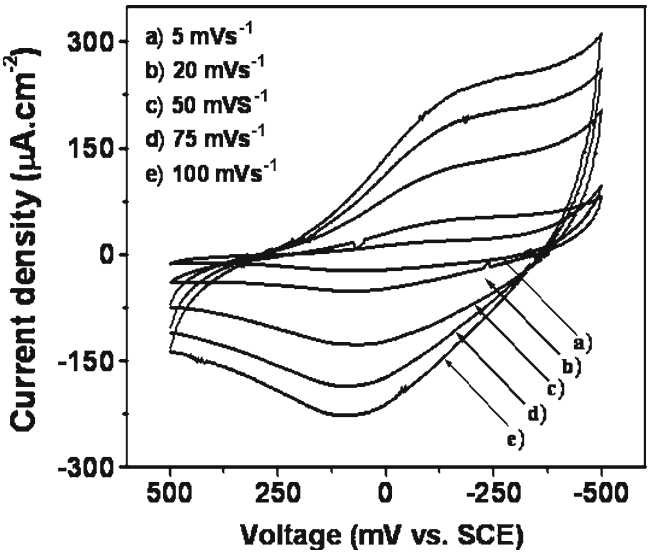

Figure 7. Variation of cyclic voltammograms at different scan rates for SnO_2:H_2O electrode with a weight of 0·22 mg cm^{-2}.

weights of SnO_2:H_2O electrode. For deposited weight of 0·03 mg cm^{-2} the electrode was unstable in Na_2SO_4 electrolyte and therefore, its C–V curve is not included in the figure. It was observed that the current under the curve increases with increase in the deposited weight and hence the capacitance increases from 6 to 13 F g^{-1} with weight increases from 0·07 to 0·22 mg cm^{-2}. At lower deposited weight, small number of electrochemically active sites present in the film results into the low capacitance value. Figure 7 shows the C–V curves with different scan rates

for the SnO_2:H_2O electrode for a deposited weight of 0·22 mg cm^{-2}. The maximum specific capacitance observed for SnO_2:H_2O electrode is 25 F g^{-1} at 5 mV s^{-1} scan rate. The nanocrystalline nature and high resistivity of the material (10^5 Ω cm) may be the causes for the low capacitance value. Hu *et al* (2007) observed that the addition of SnO_2 into RuO_2 matrix forming composite electrode increases the specific surface area and hence the specific capacitance value of RuO_2 electrode, further the porous SnO_2:H_2O electrode may be used as a substrate for chemical deposition of RuO_2 to form composite electrode, which in turn may reduce the cost and increase the specific capacitance of RuO_2 electrodes. More work on this aspect is going on.

4. Conclusions

In conclusion, nanosized thin films of hydrous tin oxide (SnO_2:H_2O) have been synthesized by simple SILAR method at room temperature. The agglomeration of nanoparticles forming porous morphology has been observed from SEM studies. The films are hydrophilic with semiconducting electrical behaviour. The electrochemical properties showed that the SnO_2:H_2O electrode has specific capacitance of 25 F g^{-1} in 0·5 Na_2SO_4 electrolyte.

Acknowledgements

One of the authors (CDL) is grateful to the All India Council for Technical Education (AICTE), New Delhi, for financial support through scheme F. No. 8023/BOR/RID/RPS-165/2009-10. Authors are also grateful to the Council for Scientific and Industrial Research (CSIR), New Delhi, for financial support through scheme no. 03(1165)/10/EMR-II.

References

Abello L, Bochu B, Gaskov A, Koudryavtseva S, Lucazeau G and Roumyantseva M 1998 *J. Solid State Chem.* **135** 78

Bockman O, Ostvold T, Voyiatzis G A and Papatheodorou G N 2000 *Hydrometallurgy* **55** 93

Burke L D and Whelan D P 1979 *J. Electroanal. Chem.* **103** 179

Burke L D, Mulcahy J K and Venkatesan S 1977 *J. Electroanal. Chem.* **81** 339

Chang S T, Leu I C and Hon M H 2005 *J. Alloys Compd* **403** 335

Dhawale D S, More A M, Latthe S S, Rajpure K Y and Lokhande C D 2008 *Appl. Surf. Sci.* **254** 3269

Hattori T, Athoh S, Tagawa T and Murakami J 1987 *Preparation of catalysts IV* (eds.) B Delmon *et al* (Amsterdam: Elsevier) p. 113

Hu C C, Chang K H and Wang C C 2007 *Electrochim. Acta* **52** 4411

Karuppuchamy S and Jeong J M 2006 *J. Oleo Sci.* **55** 263

Kostrikin A V, Spiridonov F M, Linko I V, Kosenkova O V, Kuznetsova R V and Komissarova L N 2007 *Russ. J. Inorg. Chem.* **52** 1098

Li Y, Xie X, Liu J, Cai M, Rogers J and Shen W 2008 *J. Chem. Eng.* **136** 398

Michell D, Rand D A J and Woods R 1978 *J. Electroanal. Chem.* **89** 397

Park B O, Lokhande C D, Park H S, Jung K D and Joo O S 2004a *Mater. Chem. Phys.* **87** 59

Park B O, Lokhande C D, Park H S, Jung K D and Joo O S 2004b *J. Power Sources* **134** 148

Pathan H M and Lokhande C D 2004 *Bull. Mater. Sci.* **27** 85

Pell W G and Conway B E 2001 *J. Electro. Chem.* **500** 121

Subramanian V, Hall S C, Smith P H and Rambabu B 2004 *Solid State Ionics* **175** 511

Tolstoy V P 2006 *Russ. Chem. Rev.* **75** 61

Wang Y and Herron N 1991 *J. Phys. Chem.* **95** 525

Yang L X, Zhu Y J, Tong H, Liang Z H, Li L and Zhang L 2007 *J. Solid State Chem.* **180** 2095

Zheng J P, Cygan P J and Jow T R 1995 *J. Electrochem. Soc.* **142** 2699